SUPPORTING INFORMATION

Supporting Information for

High thermoelectric performance based on $CsSnI_3$ thin films with improved stability

Weidong Tang,[a] *Tianjun Liu*[a] and *Oliver Fenwick*[a*]

[a] *School of Engineering and Materials Science, Queen Mary University of London, Mile End Road, London E1 4NS, United Kingdom;*

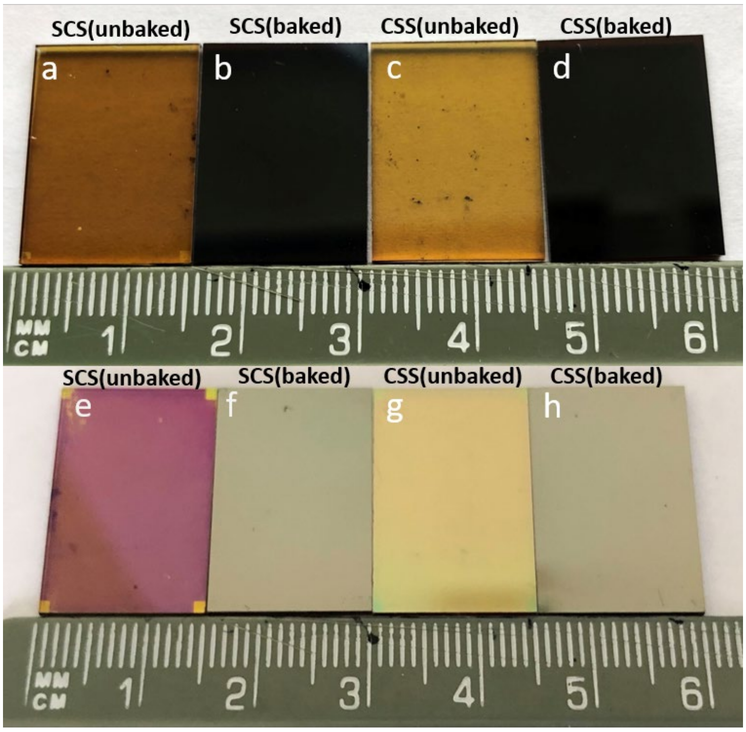

Figure S1. Optical images of the two types $CsSnI_3$ thin films before and after annealing steps. (**a-d**) Back-lit films and (**e-h**) front-lit films.

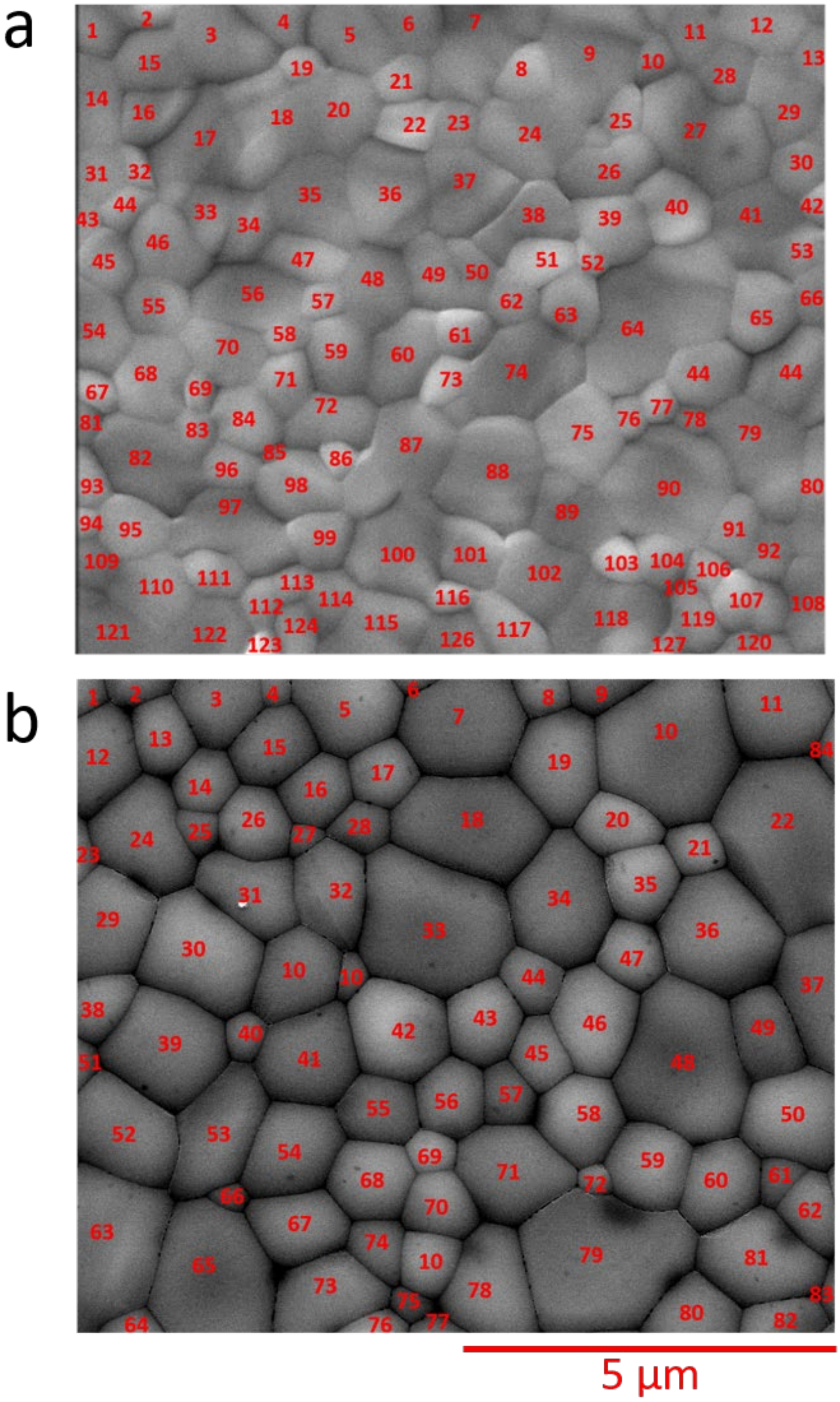

Figure S2. Grain counts and average grain size calculation of $CsSnI_3$ thin films (**a**) CSS and (**b**) SCS.

$$\text{The average grain size} = \frac{\text{total area}}{total\ number}$$

The average grain size of SCS = 1.06 µm^2

The average grain size of CSS = 0.71 µm^2

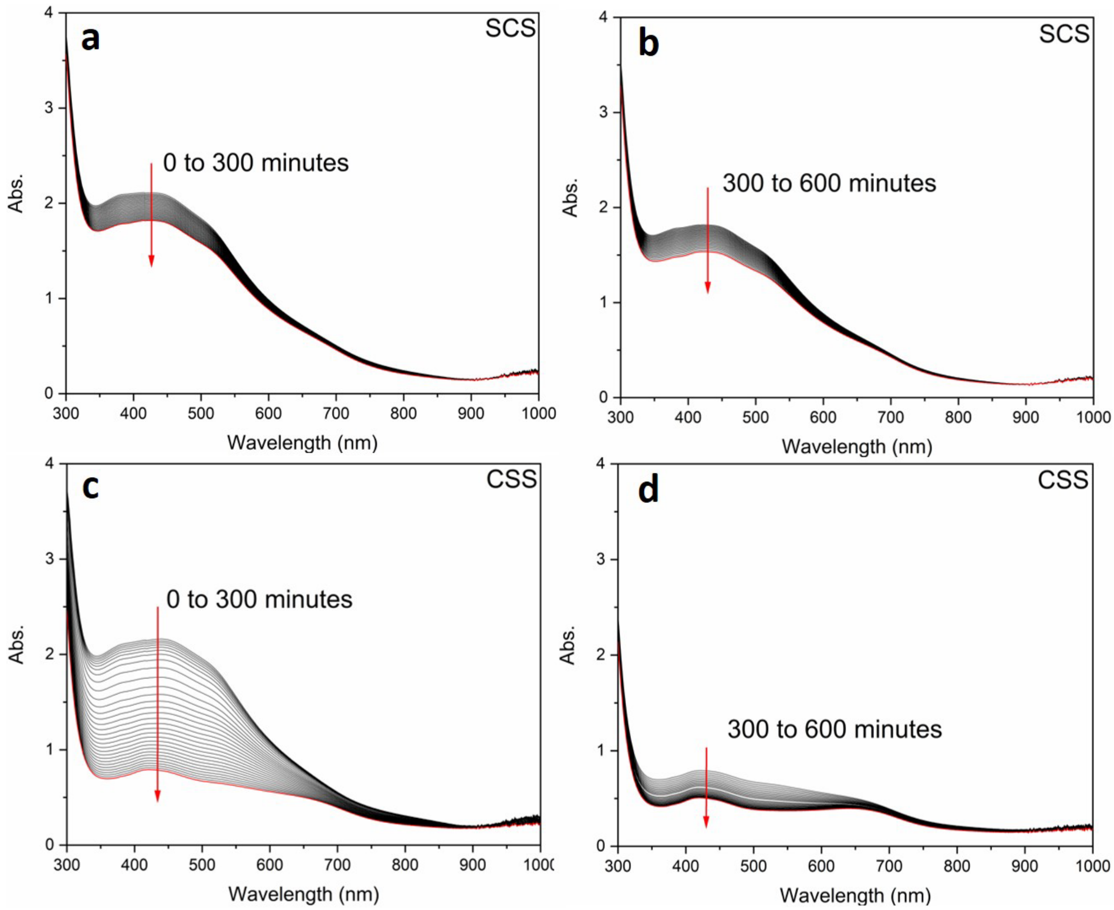

Figure S3. UV-vis absorption spectra of the two types $CsSnI_3$ thin films. Time dependent UV-vis absorption spectra of SCS $CsSnI_3$ thin films **(a)** from 0 to 300 minutes and **(b)** from 300 to 600 minutes. Time dependent UV-vis absorption spectra of CSS $CsSnI_3$ thin films **(c)** from 0 to 300 minutes and **(d)** from 300 to 600 minutes.

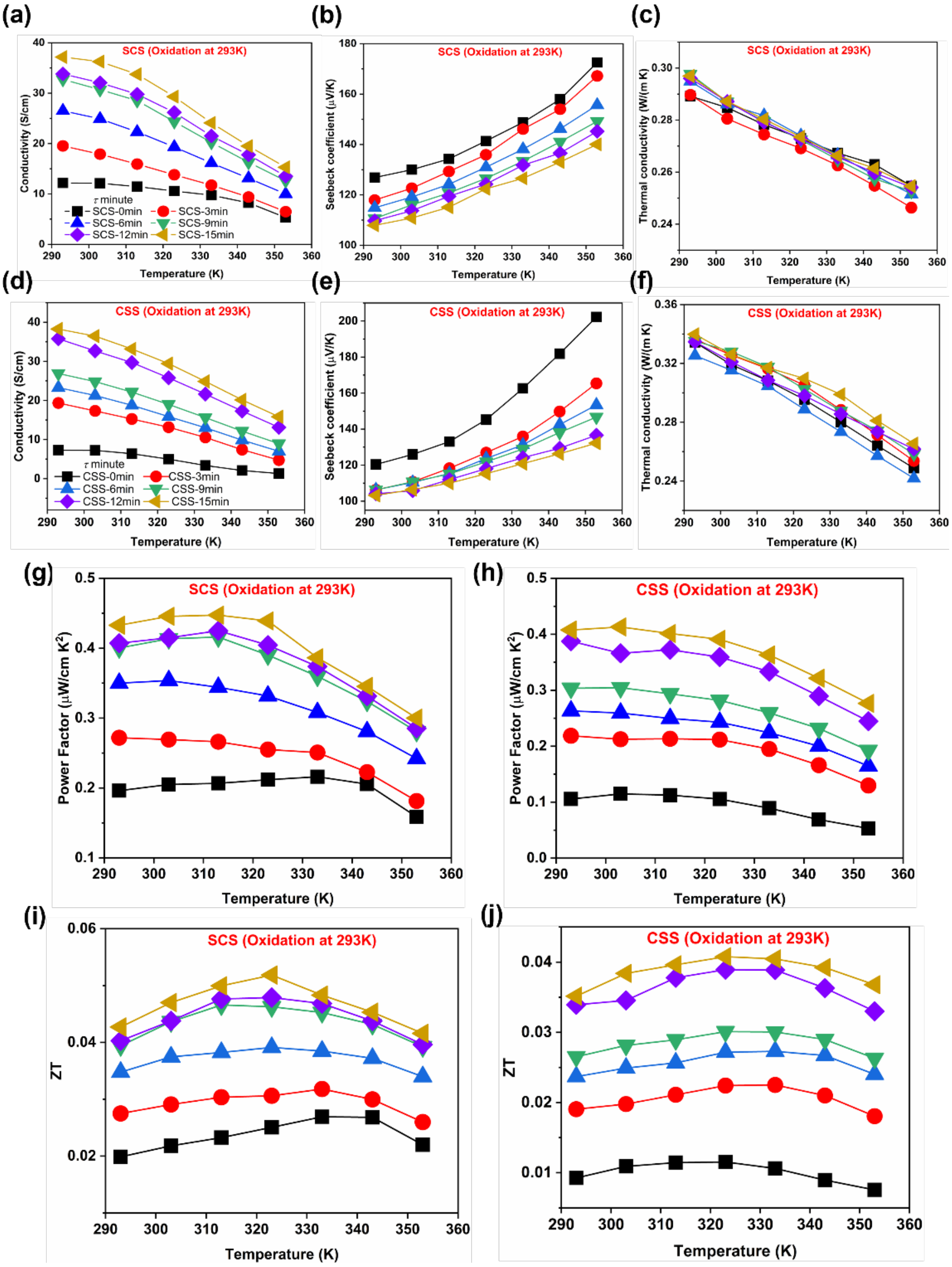

Figure S4. Thermoelectric properties of the two types $CsSnI_3$ thin films oxidised at 20 °C. Temperature dependent electrical conductivity, σ **(a)**, Seebeck coefficient, S **(b)**, thermal conductivity, κ_{total} **(c)**, power factor, PF **(g)** and figure-of-merit, *zT* **(i)**, of SCS $CsSnI_3$ thin films with air exposure at 20 °C. Temperature dependent electrical conductivity, σ **(d)**, Seebeck coefficient, S **(e)**, thermal conductivity, κ_{total} **(f)**, power factor, PF **(h)** and figure-of-merit, *zT* **(j)** of CSS $CsSnI_3$ thin films with air exposure at 20 °C.

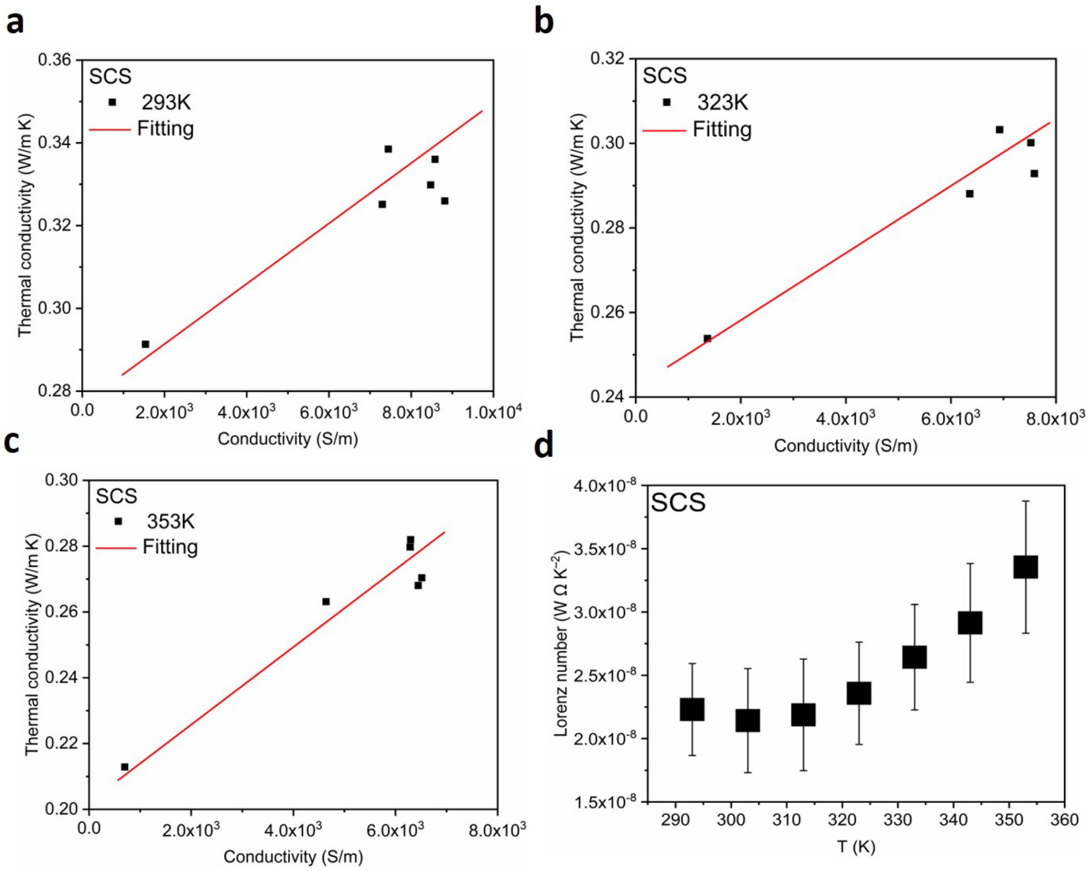

Figure S5. The relationship between thermal conductivity (total) and electrical conductivity of SCS $CsSnI_3$ thin films. (a-c) The total thermal conductivity as a function of electrical conductivity with linear fitting at 293 K, 323 K and 353 K. **(d)** Temperature dependence of Lorenz number from 293 K to 353K.

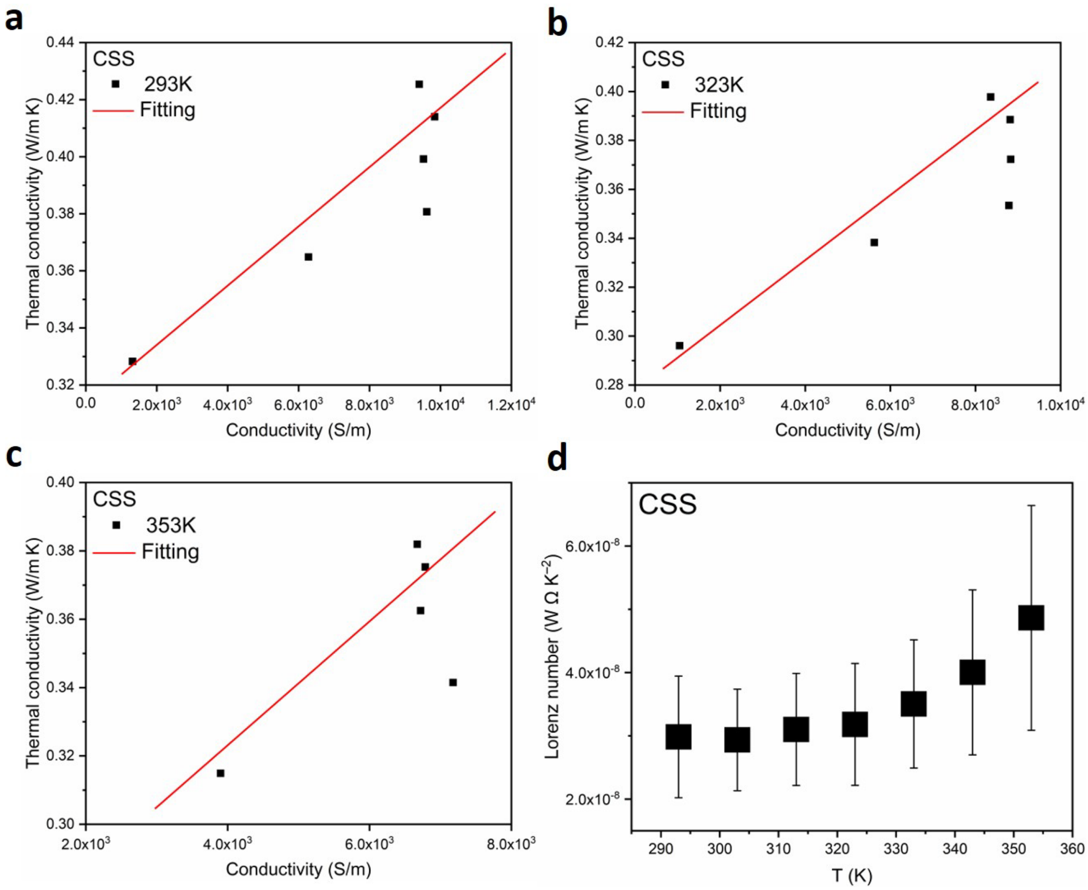

Figure S6. The relationship between thermal conductivity (total) and electrical conductivity of CSS $CsSnI_3$ thin films. (a-c) The total thermal conductivity as a function of electrical conductivity with linear fitting at 293 K, 323 K and 353 K. **(d)** Temperature dependence of Lorenz number from 293 K to 353K.

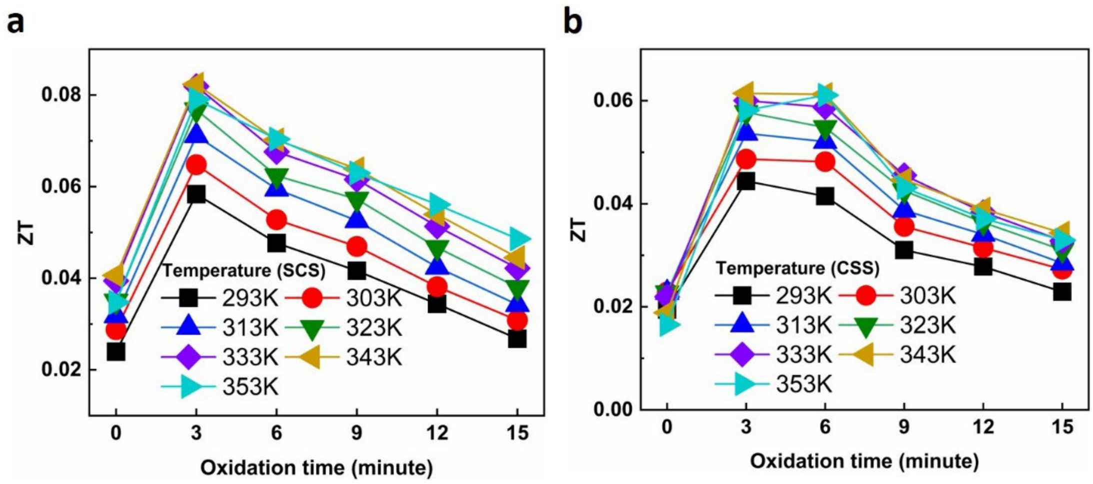

Figure S7. The Figure of merit, *zT*, stability measurement of $CsSnI_3$ thin films oxidised at 80 °C. (**a**) *zT* of a SCS film and (**b**) *zT* of a CSS film.

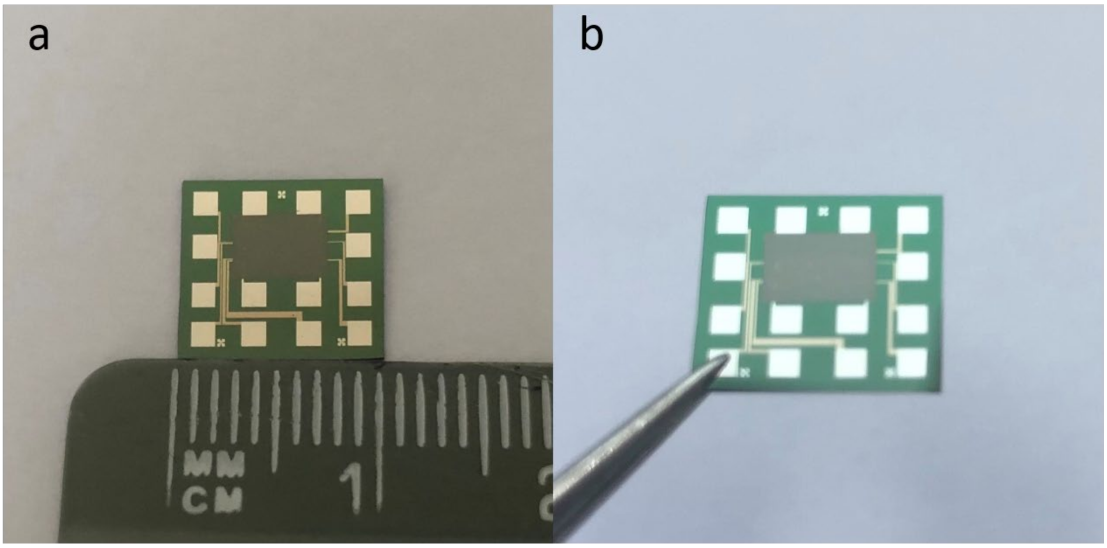

Figure S8. Images of thermoelectrical property measurement chips with deposited $CsSnI_3$ thin films.

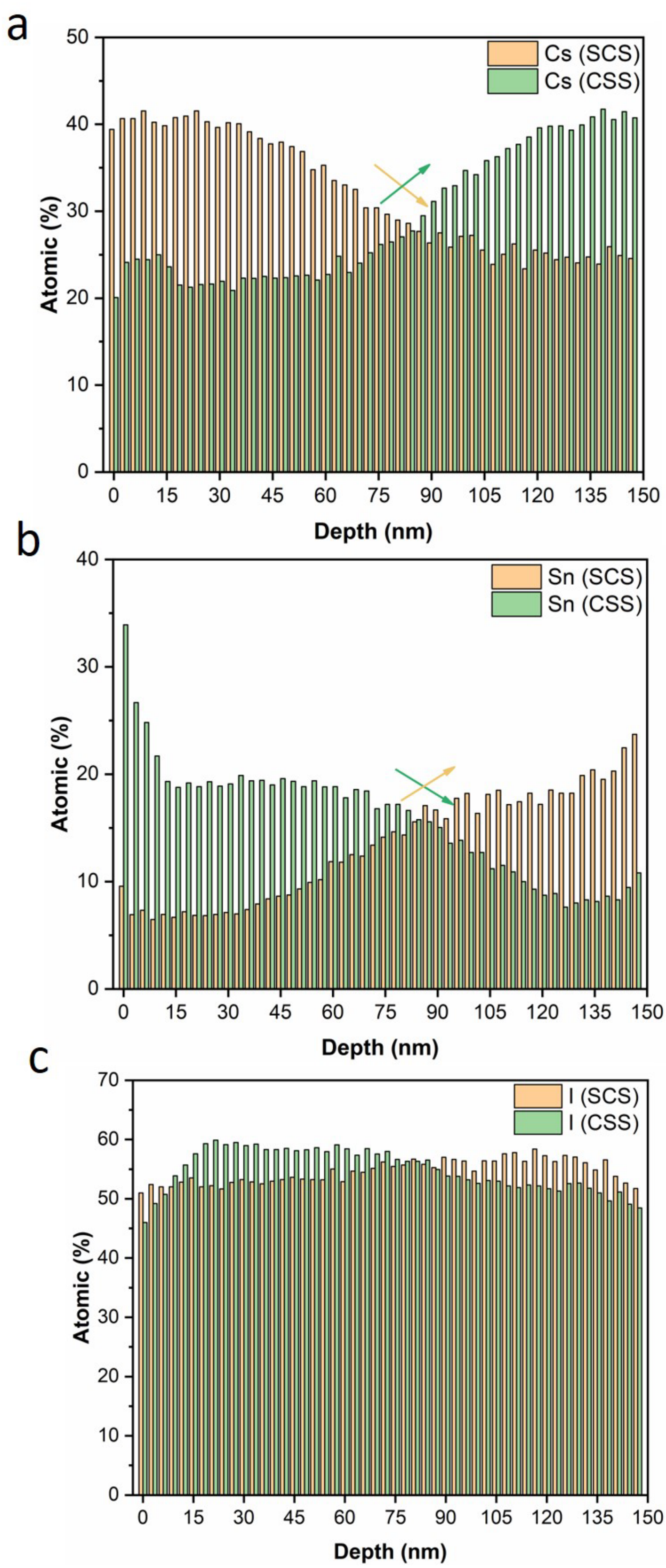

Figure S9. XPS depth profile of elemental concentration for $CsSnI_3$ thin films (from 0 to 150 nm). (**a**) Cesium (**b**) Tin (**c**) Iodide.

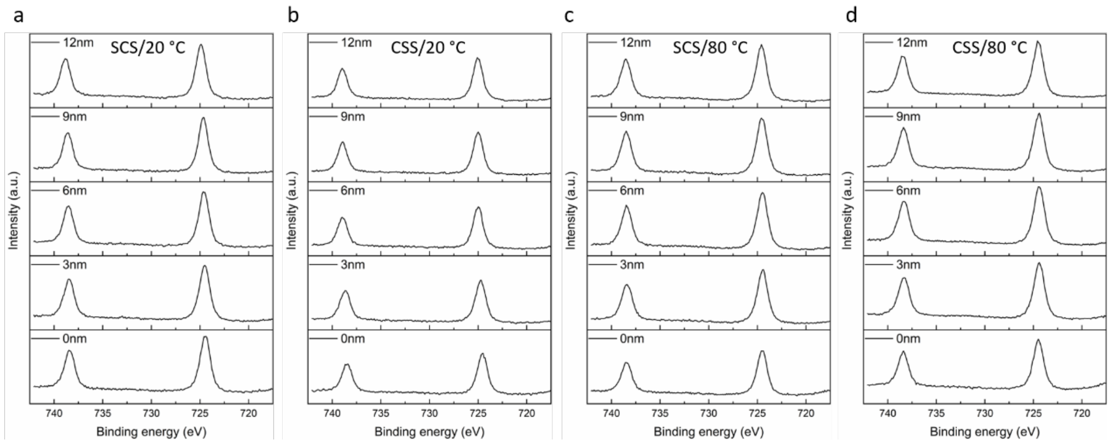

Figure S10. XPS depth profile of Cs 3d (Caesium) for $CsSnI_3$ thin films (from 0 to 12 nm). (**a**) SCS film oxidised at 20 °C (**b**) CSS film oxidised at 20 °C (**c**) SCS oxidised at 80 °C (**d**) CSS oxidised at 80 °C.

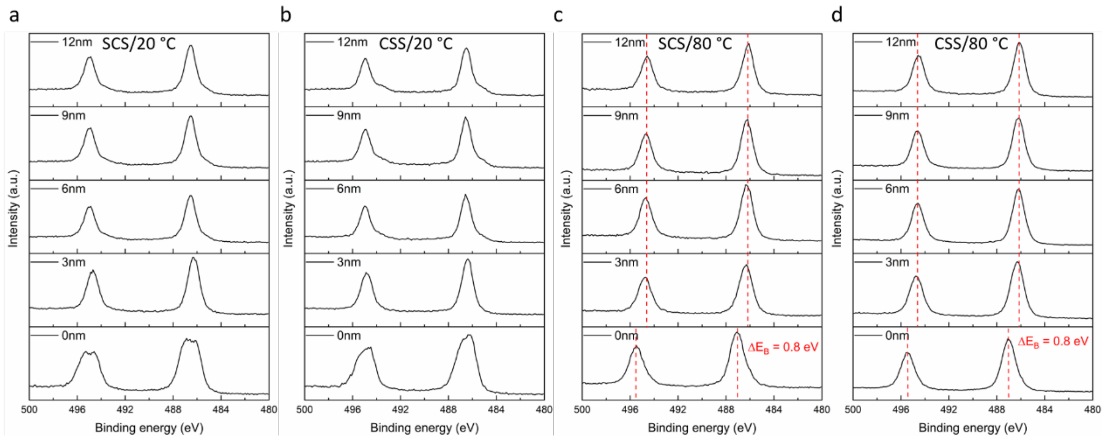

Figure S11. XPS depth profile of Sn 3d (Tin) for $CsSnI_3$ thin films (from 0 to 12 nm). (**a**) SCS film oxidised at 20 °C (**b**) CSS film oxidised at 20 °C (**c**) SCS oxidised at 80 °C (**d**) CSS oxidised at 80 °C.

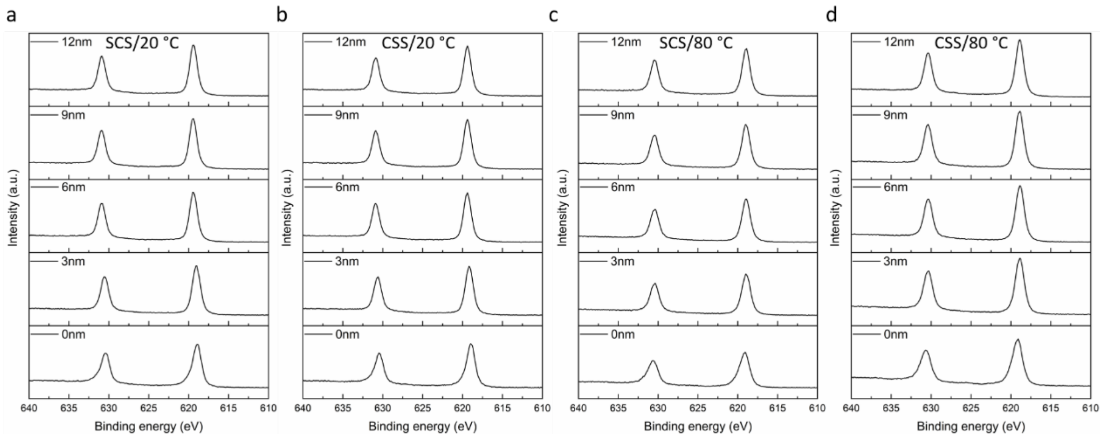

Figure S12. XPS depth profile of I 3d (Iodide) for $CsSnI_3$ thin films (from 0 to 12 nm). (**a**) SCS film oxidised at 20 °C (**b**) CSS film oxidised at 20 °C (**c**) SCS oxidised at 80 °C (**d**) CSS oxidised at 80 °C.

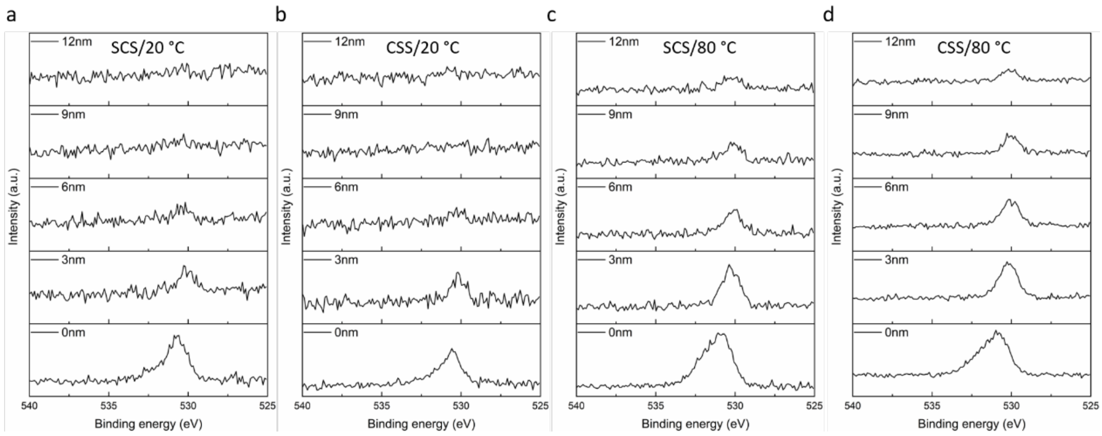

Figure S13. XPS depth profile of O 1s (Oxygen) for $CsSnI_3$ thin films (from 0 to 12 nm). (**a**) SCS film oxidised at 20 °C (**b**) CSS film oxidised at 20 °C (**c**) SCS oxidised at 80 °C (**d**) CSS oxidised at 80 °C.

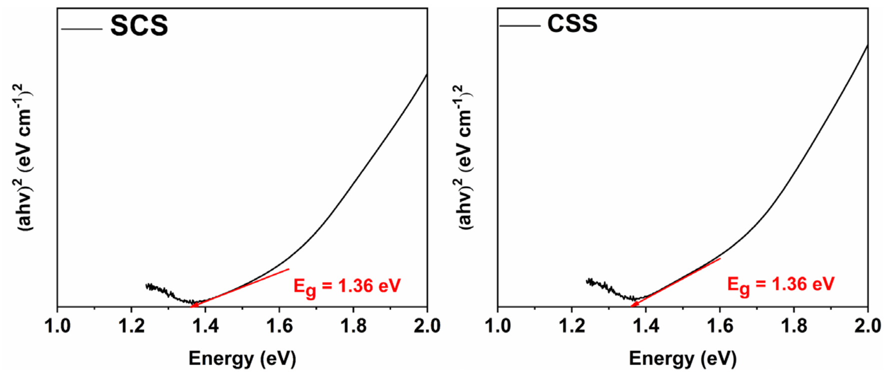

Figure S14 Tauc plots of the absorption spectra of SCS and CSS $CsSnI_3$ thin films, confirming a band gap of 1.36 eV in both cases.

Table S1: Auger peaks of reference Sn metal (Sn^0) and our $CsSnI_3$ thin films.

Sample (ev)	$M_5N_{4,5}N_{4,5}$					$M_4N_{4,5}N_{4,5}$	
	peak a	peak b				peak c	peak d
	$^1S_0$	$^1G_4$	$^3P_2$	$^3F_{2,3}$	$^3F_4$	$^1G_4\,^1D_2$	$^3F_{2,3}$
Barlow* Ref. [1]	421.3	425.6	426.8	427.9	428.7	434.1	436.3
Pessa Ref. [2]	422.9	425.6		427.6		434.1	
SCS-20(0nm)	422.5	426.4				432.7	436.1
SCS-20(3nm)	421.5	427.2				433.1	435.3
SCS-20(6nm)	421.2	427.8					435.3
SCS-20(9nm)	421.3	428					435.6
SCS-20(12nm)	421.1	428					435.5
CSS-20(0nm)	422.8	426.7				432.7	435.6
CSS-20(3nm)	421.2	427.7				433.4	435.8
CSS-20(6nm)	421.3	428.1					435.5
CSS-20(9nm)	421.3	428.3					435.6
CSS-20(12nm)	421.6	428.2					435.6
SCS-80(0nm)	422.5	425.5				432	434.7
SCS-80(3nm)	421.3	426.4				433.4	435.6
SCS-80(6nm)	421.7	426.8				433.7	435.9
SCS-80(9nm)	421.8	427.2					435
SCS-80(12nm)	421.6	428					435.6
CSS-80(0nm)	423.1	425.5				432.4	435.5
CSS-80(3nm)	421.3	426.5				433.6	436.2
CSS-80(6nm)	421.5	426.9				433.9	435.8
CSS-80(9nm)	421.6	427.2					435
CSS-80(12nm)	421.8	427.7					435.4

Table S2: Experimental binding, Auger kinetic energy values and Auger parameter for SCS and CSS films compare to references.

Sample	E_b $3d_{5/2}$ (ev)	*ΔE_b $3d_{5/2}$(oxide-metal) (ev)	E_k $M_5N_{45}N_{45}$ (ev)	*ΔE_k (oxide-metal) (ev)	α' (ev)	Ref.
Sn-metal	483.8		431.6		915.4	3
Sn-metal	484.9		430		914.9	4
SnO	486.4	2.6	426.2	5.4	912.6	4
SnO_2	487.1	3.3	424.1	7.5	911.2	4
SCS-20(0nm)	486.6	2.8	426.4	5.2	913.0	This work
SCS-20(3nm)	486.4	2.6	427.2	4.4	913.6	This work
SCS-20(6nm)	486.6	2.8	427.8	3.8	914.4	This work
SCS-20(9nm)	486.6	2.8	428.0	3.6	914.6	This work
SCS-20(12nm)	486.6	2.8	428.0	3.6	914.6	This work
CSS-20(0nm)	486.4	2.6	426.7	4.9	913.1	This work
CSS-20(3nm)	486.5	2.7	427.7	3.9	914.2	This work
CSS-20(6nm)	486.6	2.8	428.1	3.5	914.7	This work
CSS-20(9nm)	486.6	2.8	428.3	3.3	914.9	This work
CSS-20(12nm)	486.6	2.8	428.2	3.4	914.8	This work
SCS-80(0nm)	487.1	3.3	425.5	6.1	912.6	This work
SCS-80(3nm)	486.3	2.5	426.4	5.2	912.7	This work
SCS-80(6nm)	486.4	2.6	426.8	4.8	913.2	This work
SCS-80(9nm)	486.2	2.4	427.2	4.4	913.4	This work
SCS-80(12nm)	486.3	2.5	428.0	3.6	914.3	This work
CSS-80(0nm)	487.1	3.3	425.5	6.1	912.6	This work
CSS-80(3nm)	486.3	2.5	426.5	5.1	912.8	This work
CSS-80(6nm)	486.2	2.4	426.9	4.7	913.1	This work
CSS-80(9nm)	486.2	2.4	427.2	4.4	913.4	This work
CSS-80(12nm)	486.1	2.3	427.5	3.9	913.8	This work

Supporting References

1. S. Barlow, P. Bayat-Mokhtari and T. E. Gallon, *Journal of Physics C: Solid State Physics*, 1979, **12**, 5577-5584.
2. M. Pessa, S. Aksela and M. Karras, *Physics Letters A*, 1970, **31**, 382-383.
3. A. F. Lee and R. M. Lambert, *Physical Review B*, 1998, **58**, 4156-4165.
4. L. Kövér, Z. Kovács, R. Sanjinés, G. Moretti, I. Cserny, G. Margaritondo, J. Pálinkás and H. Adachi, *Surface and Interface Analysis*, 1995, **23**, 461-466.